Resonant coupling of molecular excitons and optical anapoles in silicon nanosphere-J-aggregate heterostructure under vector beam illumination

BRIGHTON COE, ROBERT SEVIK, MAHUA BISWAS AND UTTAM MANNA*

Department of Physics, Illinois State University, Normal, Illinois 61709, USA
**umanna@ilstu.edu*

Abstract: Resonant excitation of high-index dielectric nanostructures, and their coupling with molecular excitons provide great opportunities for engineering adaptable platforms for hybrid functional optical devices. Here, we numerically calculate resonant coupling of nonradiating anapole states to molecular excitons within silicon nanosphere-J-aggregate heterostructures under illumination with radially polarized cylindrical vector beams. The results show that the resonance coupling is accompanied by a scattering peak around the exciton transition frequency, and the anapole state splits into a pair of anti-crossing eigenmodes with a mode splitting energy ≈ 200 meV. We also investigate the resonance coupling as a function of the J-aggregate parameters, such as thickness, exciton transition line width, and oscillator strength. Resonant coupling of the anapole states and J-aggregate heterostructures could be a promising platform for future nanophotonic applications such as in information processing and sensing.

1. Introduction

It is well known that the localized surface plasmon resonance (LSPR) of a metal nanostructure can strongly couple with molecular excitons in the form of a J-aggregate dye [1-10]. These metal nanostructures and molecular exciton heterostructures, termed as plexcitons [2-5] can provide unique adaptable platforms for the design and implementation of hybrid functional optical devices, such as in chemical sensors [11], pH meters [12], light harvesting [13], and other optically active devices [14, 15]. In these plexcitonic devices, the highly enhanced electric field near the surface of the nanostructures, known as "hot spot," can strongly polarize the J-aggregates, which in turn affect the plasmon oscillations of the metal nanostructures. The coupling between the molecular excitons and optical resonators can be classified into two regimes – weak and strong coupling – depending upon the coupling strength. In the weak coupling regime, the presence of an optical resonator can modify the local optical density of states, and thereby modify the spontaneous decay [16]. On the other hand, in the strong coupling regime, the coherent energy transfer between the molecular excitons and J-aggregates results in mode splitting or quantized quenching dips in the optical spectra of the plexcitons, and the mode splitting is found to undergo an anticrossing behavior with a splitting energy in the order of hundreds of meV [1, 3, 7, 17-22].

In recent years, high refractive dielectric nanostructures have attracted considerable attention as an alternative to plasmonic nanostructures because of their reduced dissipative losses and large enhancement of both the electric and magnetic near fields [23-26]. More specifically, it has been shown that dielectric nanostructures can be promising candidates to tailor light-matter interactions at the nanoscale, such as in the enhancement of quantum emitters photoluminescence [24, 27], strong coupling and Rabi splitting in silicon (Si) nanosphere-J-aggregate core-shell heterostructures [22], *etc*. In this regard, the discovery of the electrodynamic anapole state as a non-radiating source in high-index dielectric materials provides a unique playground to realize novel nanophotonic devices [28-33].

For time-varying oscillating charge-current distributions, in the long-wavelength approximation, the electrodynamic anapoles are related to the superposition of the scattered

fields of conventional and toroidal dipoles, given by [28, 29], $\boldsymbol{P} = -ik\boldsymbol{T}$. This means, the far-field radiation will vanish if the contributions of the Cartesian electric ($\boldsymbol{P}$) and toroidal dipoles ($\boldsymbol{T}$) to the scattered field are *equal* and *out-of-phase* [28-30]. Therefore, excitation of optical anapoles is characterized by dips or minima in the scattering spectra. However, isotropic nanostructures are not suitable for the excitation of anapole mode under plane wave (PW) illumination because along with the Cartesian electric and toroidal dipoles, other adjacent modes, such as magnetic dipoles, electric and magnetic quadrupoles, *etc*. are also excited. Therefore, the scattering minima associated with the excitation of optical anapoles are not possible to detect for spherical geometry under PW illumination. As a result, excitation of optical anapoles relies on the design of highly specialized structures (such as nanodisks) [28], in which the dominant contribution comes from the electric dipole mode, while all other modes are strongly suppressed. On the other hand, radially polarized cylindrical vector beams can selectively excite only electric multipoles (no magnetic multipoles), and thereby allow for the excitation of an anapole state within the nanospheres without relying on the design of specialized structures. Recently, we demonstrated that the radially polarized cylindrical vector beams (CVBs) can selectively excite only electric multipoles (no magnetic multipoles) [34], and thereby allow for the excitation of an anapole state within the nanospheres [29].

Not long ago, Liu *et. al*.[35] theoretically demonstrated resonance coupling between the exciton transition and the anapole state within a heterostructure composed of a Si *nanodisk* and a molecular J-aggregate ring under PW illumination. The results showed that instead of a quenching dip, a scattering peak is generated around the exciton transition frequency for the heterostructures, and the anapole state splits into a pair of eigenmodes characterized as pronounced dips in the scattering spectra [35]. Moreover, an anticrossing behavior with a mode splitting of ≈ 161 meV was observed indicating that a strong coupling regime can be achieved for coupling between the exciton transition and the anapole state [35].

Here, using Finite Difference Time Domain (FDTD) [36] method, we numerically calculate the resonance coupling between the exciton transition and the anapole state within Si *nanosphere* and molecular J-aggregate heterostructures under tightly-focused *radially* polarized (RP) CVB illumination. The RP illumination selectively excites the electric multipolar resonances within the Si nanosphere, and the interference of electric and toroidal dipolar modes with the same amplitude but out of phase results in excitation of anapole states within the Si nanospheres for a specific wavelength. We find that, similar to Si *nanodisk* and J-aggregate heterostructures [35], the resonance coupling between the anapole state and exciton within Si nanosphere and J-aggregate heterostructures is accompanied by a scattering peak instead of a dip around the exciton transition frequency. At this frequency, the anapole state splits into a pair of eigenmodes characterized by pronounced dips within the scattering spectra. The mode splitting is found to undergo an anticrossing behavior with a mode splitting energy ~ 200 meV for Si *nanosphere* and J-aggregate heterostructures under radial beam illumination, which is ~ 25% higher than the mode splitting energy of 161 meV associated with Si *nanodisk* and J-aggregate heterostructures [35]. Therefore, our results demonstrate that a stronger resonance coupling between the anapole state and exciton resonance could be achieved within Si *nanosphere* and J-aggregate heterostructures under radial beam illumination. We also investigate the resonance coupling within Si nanosphere and J-aggregate heterostructures for varying J-aggregate thickness, exciton transition line width, and oscillator strength.

2. Results and Discussion

2.1 The scheme

As mentioned above, the field distributions of the tightly-focused CVBs can be used to selectively excite and enhance multipolar resonances [34], and thereby excite anapole states within the nanospheres [29]. CVBs are solutions of Maxwell's equations that possess spatially

varying polarization with cylindrical symmetry in both amplitude and phase [37]. The CVBs can have the electric field aligned in the radial (radially polarized beams) or azimuthal directions (azimuthally polarized beams), while the magnetic field is aligned in the azimuthal or radial directions, respectively with respect to the optical axis. A number of active and passive methods [38-42], including interferometric method [40, 42], liquid-crystal based method [41], *etc*. have been used to generate CVBs. Moreover, the spatially varying polarization properties of CVBs have been previously used to tailor multipolar electric and magnetic resonances [29, 34, 43-46], and excite dark mode and Fano resonances [47-49] in metallic and dielectric nanostructures; perform optical imaging [50-52], and optical trapping [53] of plasmonic particles; morphology conversion of surface microstructures [54], *etc*. Here, we investigate resonant coupling of anapole states to molecular excitons within Si nanosphere-J-aggregate heterostructures under illumination with tightly-focused RP beam (Numerical aperture, NA = 0.95) as shown in Fig. 1. For our calculations, the J-aggregate molecules were distributed in a way such that the silicon nanospheres and the J-aggregates formed a core-shell structure while the J-aggregates formed a film on the substrate as shown in Fig. 1. This geometry was chosen to mimic the experimental structures that can be produced by spin casting. The tightly focused radially polarized beam is expected to selectively excite the electric and toroidal dipolar resonances in Si nanosphere-J-aggregate heterostructures, and thereby lies the possibility of a coherent energy transfer between the molecular excitons and J-aggregates. For creating a tightly-focused radially polarized beam in the simulation, we used a k-space beam profile approach [55]. The k-space beam profile is based on the method of using a classical diffraction theory to calculate the effects of high numerical aperture on the focusing of coherent light.

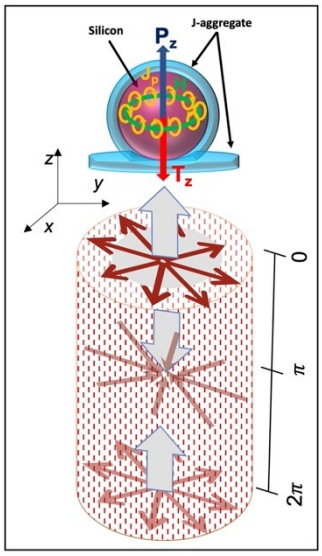

Fig. 1. The scheme showing the excitation of a Si nanosphere-J-aggregate heterostructure under tightly-focused radially polarized beam excitation with numerical aperture, NA = 0.95. The J-aggregate molecules were distributed in a way such that the nanosphere and the J-aggregate formed a core-shell structure while the J-aggregate formed a film on the substrate. The tightly focused beam was created using a k-space beam profile approach [55]. (Color online only)

2.2 Resonance coupling between the anapole state and molecular excitons

To investigate the resonance coupling between the optical anapoles and molecular excitons, we have calculated the scattering spectra of a single Si nanospheres, J-aggregate only ring/film, and J-aggregate-Si nanosphere heterostructures as shown in Fig. 2. The simulated structure is shown in Fig. 1. For this calculation, to account for the J-aggregate exciton, the dielectric permittivity is described with a classical one-oscillator Lorentzian model,

$$\varepsilon_J(\omega) = \varepsilon_\infty - \frac{f\omega_0^2}{\omega^2 - \omega_0^2 + i\omega\gamma}, \quad (1)$$

where ε_∞ denotes the high-frequency component of the dielectric function of the J-aggregates/ polyvinyl alcohol (PVA) mixture (set to 2.5) (PVA is used to bind the J-aggregate on the surface of the nanospheres), ω_0 is the exciton transition frequency, γ is the exciton line width (set to 58 meV), and f is the oscillator strength (varied from 0.2 to 0.4, depends on molecular concentration) [22]. In our previous studies, we have shown that the excitation of a nanosphere using azimuthally polarized beam excites only the magnetic modes. On the contrary, for RP beam illumination, only the electric modes are excited within the nanosphere [34], and thereby allow for the excitation of an anapole state within the nanospheres [29]. The dips in the scattering spectra observed at wavelength, $\lambda \approx 485$ nm, and $\lambda \approx 495$ nm corresponding to the single Si nanospheres of $d = 160$ nm, and 220 nm, as shown in Figs. 2a and 2d (blue curves), respectively are signature of anapole states that appear under RP beam illumination.

Figs. 2a and 2d also show the scattering intensity of single nanosphere-J-aggregate heterostructures with the J-aggregate thickness, $t \sim 20$ nm, and nanosphere diameter, $d = 160$ nm, and 220 nm, respectively for oscillator strengths, $f = 0.2$ (red curves) and 0.4 (green curves) under RP beam illumination. In this calculation, the exciton transition frequency was set to anapole frequency ($\lambda \approx 485$ nm for $d = 160$ nm, and $\lambda \approx 495$ nm for $d = 220$ nm), which can be tuned by varying the diameter of the Si nanosphere to match the exciton transition frequency of the J-aggregate for various applications. Therefore, depending upon the excitation transition frequency of a specific J-aggregate, the anapole frequency can be tuned accordingly. For practical purposes, a number of J-aggregates can be used. For example, Cyanine dye in a PVA matrix ($\lambda_{ex} \approx 693$ nm) [4], TDBC dye in PVA matrix ($\lambda_{ex} \approx 593$ nm) [22], *etc*. have been used to investigate resonance coupling within plexcitonic systems in the optical regime. Nevertheless, one can clearly see the appearance of a scattering peak around the exciton transition frequency and the splitting of an anapole state of the nanosphere into a pair of scattering dips with the splitting enlarged as f increases, as indicated by the dashed circle region in Figs. 2a and 2d for nanosphere diameter, $d = 160$ nm, and 220 nm, respectively. These results indicate a strong resonance coupling between the optical anapoles and J-aggregate molecular excitons under RP beam illumination.

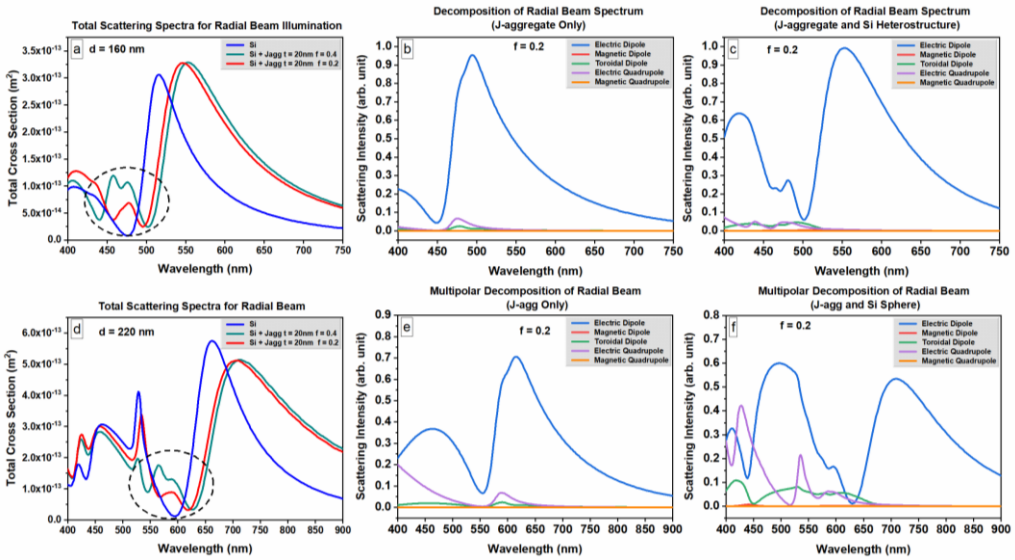

Fig. 2. (a) and (d) show scattering intensity of the heterostructures for Si diameter, $d = 160$ nm, and 220 nm, respectively and J-aggregate thickness, $t = 20$ nm, and oscillator strengths, $f = 0.2$ and 0.4. (b) and (e) show the multipolar decomposition of the scattering spectra of J-aggregate

only for J-aggregate inner diameter of 160 nm, and 220 nm respectively with t = 20 nm, f = 0.2. (c) and (f) show the multipolar decomposition of the scattering spectra and J-aggregate-Si nanosphere heterostructure for Si diameter, d = 160 nm, and 220 nm, respectively, with t = 20 nm, and f = 0.2 under radially polarized beam illumination. (Color online only)

To understand the origin of this coupling and splitting of the anapole states, we have performed multipolar decomposition of the scattering spectra of the J-aggregates only (Figs. 2b and 2e), and J-aggregate-nanosphere heterostructures (Figs. 2c and 2f), for f = 0.2. The results show that the scattering from both the J-aggregates only and J-aggregate-nanosphere heterostructures are dominated by the contributions from the electric and toroidal dipolar resonances with some contributions from electric quadrupole resonances. Since the anapole state of the Si nanosphere is caused by the destructive interference of the Cartesian electric and toroidal dipolar moments [28, 29], the splitting of the anapole state of the heterostructure can also be attributed to the coupling of the Cartesian electric and toroidal dipolar moments between the Si nanosphere and J-aggregate. This mechanism is similar to the coupling of the Cartesian electric and toroidal moments between the Si nanodisk and the J-aggregate ring under PW illumination [35]. The electric quadrupole resonance also contributes to the scattering dip for the heterostructure (purple line). As a result, there is a slight shift between the scattering dip and the crossing point of the Cartesian electric and toroidal dipole moments, which is similar to the contributions from magnetic quadrupole resonance for coupling between the Si nanodisk and the J-aggregate ring [35].

2.3 Anticrossing behavior and Rabi splitting in heterostructures

The coupling between molecular excitons and optical anapoles can result in an anticrossing of the dispersion curves and the formation of two hybrid energy states separated by a Rabi splitting, similar to the plasmon-exciton coupling in plexcitonic systems [1, 3, 7, 17-22]. The Rabi splitting values can be extracted using a coupled oscillator model, where the energies of the upper band (UB) and lower band (LB) can be written as [4, 56],

$$E_{UB,LB}(\hbar\omega_a) = \frac{\hbar\omega_a+\hbar\omega_e}{2} \pm \frac{1}{2}\sqrt{4g^2 + (\hbar\omega_a - \hbar\omega_e)^2} \qquad (2)$$

where $\hbar\omega_a$ and $\hbar\omega_e$ are the energies of the optical anapole and exciton transition, g is the transition rate, and the Rabi splitting energy ($\hbar\Omega_R = 2g$) can be obtained when $\hbar\omega_a = \hbar\omega_e$. Figs. 3a and 3b show the energy diagrams associated with the scattering of Si nanosphere, and nanosphere-J-aggregate heterostructure, respectively, that were calculated by varying the diameter of the Si nanospheres (d = 120 to 200 nm), thereby tuning the energy of the anapole states across the exciton transition frequency, for f = 0.2 under RP beam illumination. The energy diagram of Si nanosphere (Fig. 3a) shows that the energy of the anapole state varies linearly with increasing diameter (energy) (white dashed dotted line). The energy diagram of the heterostructure (Fig. 3b) shows a distinct anticrossing behavior when the anapole energy is varied across the exciton transition energy. Note that this anticrossing behavior and the associated mode splitting are not specific to anapole states, rather this has been previously observed for resonant coupling in the plexcitonic systems [1, 3, 7, 17-22]. However, instead of scattering peaks as observed for resonant coupling in plexcitonic systems, scattering dips appear in the energy diagram, which is termed as UB and LB hybrid anapole states for resonant coupling of molecular excitons and anapole states. The energy diagram of Fig. 3b was fitted with Eq. (2) as indicated by the green curve for UB and cyan curve for LB in Fig. 3b. The fitting results show the Rabi splitting energy is approximately 200 meV as shown by the black double-sided arrow in Fig. 3b. This value is approximately 25% higher than that of the mode splitting energy of 161 meV associated with Si *nanodisk* and J-aggregate heterostructures under PW illumination [35]. Furthermore, a splitting energy of 200 meV is amongst the highest values reported for single nanoparticles [1-10].

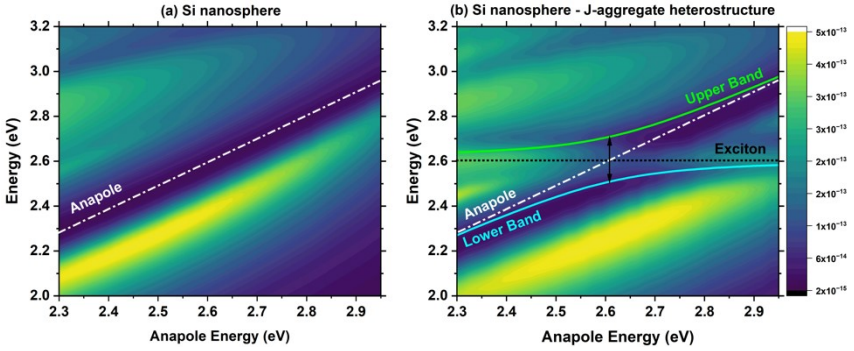

Fig. 3. Energy diagrams associated with the scattering of (a) Si nanosphere, and (b) nanosphere-J-aggregate heterostructure that were calculated by varying the diameter of the Si nanospheres (d = 120 to 200 nm) for f = 0.2. The energy diagram of the heterostructure (b) shows a distinct anticrossing behavior with a Rabi splitting energy ≈ 200 meV as indicated by the double-sided black arrow. (Color online only)

2.4 Tuning the resonance coupling between the anapoles and molecular excitons

The resonance coupling between the anapoles and molecular excitons in the nanosphere-J-aggregate heterostructures is governed by the optical response of the anapoles as well as the molecular excitons of the J-aggregates. Therefore, the J-aggregate parameters, such as thickness (t), exciton transition line width (γ), and oscillator strength (f) play a critical role in resonance coupling between the optical anapoles and molecular excitons. Figs. 4(a-c) show the scattering spectra of nanosphere-J-aggregate heterostructures for nanosphere diameter, d = 160 nm for different values of J-aggregate thickness ($0 \leq t \leq 100\,nm$), exciton transition line width ($10 \leq \gamma \leq 150\,nm$), and oscillator strength ($0.01 \leq f \leq 1.0$), respectively.

Although the near-fields associated with the optical anapoles have finite penetration depth, the field enhancements can extend into the J-aggregate ring [35]. Increasing the J-aggregate thickness, t, results in a larger quantity of molecules participating in the resonance coupling. Consequently, a stronger coupling between the optical anapoles and molecular excitons can be obtained with increasing J-aggregate thickness as evident by larger splitting of the LB and UB hybrid modes as shown in Fig. 4a (calculated for d = 160 nm, γ = 58 meV, f = 0.2). The resonance energy of the LB is found to continuously red shift with increasing thickness as expected [35]. On the other hand, the resonance energy of the UB initially blue-shifts as expected [35], but then continues to red-shift. This can be attributed to the weaker resonance coupling between the outermost molecules and optical near-fields as well as stronger radiative damping with increasing J-aggregate thickness. As a result, the UB hybrid mode becomes weaker and narrower as shown in Fig. 4a.

The scattering spectra of the heterostructure with varying excitation transition line width, γ reveal that the peak intensity of the exciton transition resonance of the J-aggregate ring decreases with increasing γ, and UB and LB resonance hybrid energy modes broaden and for γ > 75 meV, the two resonance modes merge as shown in Fig. 4b. An increase in γ results in reduced intensity of the exciton transition resonance, and the scattering peak that separates the UB and LB hybrid modes become shallower because of increased damping [35]. Therefore, with increased line width, at an upper limit (~ 75 meV in our case), the resonance coupling can no longer compete with the dissipation and therefore the coupling is no longer observed.

Fig. 4c shows the scattering spectra of the heterostructure for varying oscillator strength, f. The results show that the scattering peak intensity around the exciton transition becomes stronger and wider, and the splitting between the UB and LB resonance hybrid energy mode increases with increasing f. This can be attributed to the stronger resonance coupling between the exciton transition and optical anapoles resulting from increasing molecular concentration, and thereby stronger transition dipole moments with increasing f [35].

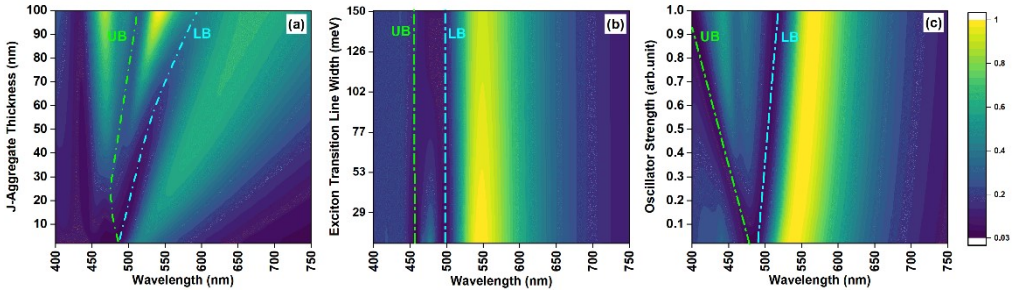

Fig. 4. Scattering spectra of nanosphere-J-aggregate heterostructures for nanosphere diameter, d = 160 nm for different values of (a) J-aggregate thickness ($0 \leq t \leq 100\ nm$), (b) exciton transition line width ($10 \leq \gamma \leq 150\ nm$), and (c) oscillator strength ($0.01 \leq f \leq 1.0$). (Color online only)

3. Conclusions

In conclusion, we have numerically calculated the resonance coupling between the exciton transition and the anapole state within a Si nanosphere and a molecular J-aggregate heterostructure under tightly focused radially polarized cylindrical vector beam illumination. We find that the anapole state and exciton resonance couple strongly within Si nanosphere-J-aggregate heterostructures, and the resonance coupling is accompanied by scattering peaks around the exciton transition frequency. We also find that the anapole state splits into a pair of eigenmodes characterized as pronounced scattering dips, and the mode splitting undergoes an anticrossing behavior with a splitting energy ≈ 200 meV. This mode splitting energy is ~ 25% higher than the mode splitting energy of 161 meV associated with Si nanodisk and J-aggregate heterostructures. Our results demonstrate that a stronger resonance coupling between the anapole state and exciton resonance could be achieved within Si nanosphere and J-aggregate heterostructures under radial beam illumination. In solid state systems made up of quantum emitters or single molecules and an optical cavity, the quantum nature of the quantum-dot–cavity system and single-molecule-cavity system has been demonstrated in the strong-coupling regime [57, 58], which could be beneficial for future applications, such as in information processing and sensing. Therefore, resonant coupling of the anapole states and heterostructures could be a promising platform nanophotonic applications such as in information processing and sensing in future.

Acknowledgments. This material is based upon work supported by the National Science Foundation (NSF) under Grant No. DMR-2208240.

Disclosures. The authors declare no conflicts of interest.

Data availability. Data underlying the results presented in this paper are not publicly available at this time but may be obtained from the authors upon reasonable request.

References

1. G. P. Wiederrecht, G. A. Wurtz, and J. Hranisavljevic, "Coherent coupling of molecular excitons to electronic polarizations of noble metal nanoparticles," Nano Lett. **4**, 2121-2125 (2004).
2. N. T. Fofang, N. K. Grady, Z. Fan, A. O. Govorov, and N. J. Halas, "Plexciton dynamics: exciton-plasmon coupling in a J-aggregate-Au nanoshell complex provides a mechanism for nonlinearity," Nano Lett. **11**, 1556-1560 (2011).
3. N. T. Fofang, T. H. Park, O. Neumann, N. A. Mirin, P. Nordlander, and N. J. Halas, "Plexcitonic nanoparticles: plasmon-exciton coupling in nanoshell-j-aggregate complexes," Nano Lett. **8**, 3481-3487 (2008).
4. A. E. Schlather, N. Large, A. S. Urban, P. Nordlander, and N. J. Halas, "Near-field mediated plexcitonic coupling and giant rabi splitting in individual metallic dimers," Nano Lett. **13**, 3281-3286 (2013).
5. F. Nan, Y.-F. Zhang, X. Li, X.-T. Zhang, H. Li, X. Zhang, R. Jiang, J. Wang, W. Zhang, L. Zhou, J.-H. Wang, Q.-Q. Wang, and Z. Zhang, "Unusual and tunable one-photon nonlinearity in gold-dye plexcitonic Fano systems," Nano Lett. **15**, 2705-2710 (2015).
6. W. H. Ni, T. Ambjornsson, S. P. Apell, H. J. Chen, and J. F. Wang, "Observing plasmonic-molecular resonance coupling on single gold nanorods," Nano Lett. **10**, 77-84 (2010).
7. P. Vasa, W. Wang, R. Pomraenke, M. Lammers, M. Maiuri, C. Manzoni, G. Cerullo, and C. Lienau, "Real-time observation of ultrafast rabi oscillations between excitons and plasmons in metal nanostructures with J-aggregates," Nat. Photonics **7**, 128-132 (2013).
8. A. Manjavacas, F. J. Garcia de Abajo, and P. Nordlander, "Quantum plexcitonics: strongly interacting plasmons and excitons," Nano Lett. **11**, 2318-2323 (2011).
9. B. G. DeLacy, O. D. Miller, C. W. Hsu, Z. Zander, S. Lacey, R. Yagloski, A. W. Fountain, E. Valdes, E. Anquillare, M. Soljacic, S. G. Johnson, and J. D. Joannopoulos, "Coherent plasmon-exciton coupling in silver platelet-j-aggregate nanocomposites," Nano Lett. **15**, 2588-2593 (2015).
10. G. Zengin, M. Wersall, S. Nilsson, T. J. Antosiewicz, M. Kall, and T. Shegai, "Realizing strong light-matter interactions between single-nanoparticle plasmons and molecular excitons at ambient conditions," Phys. Rev. Lett. **114**, 157401 (2015).
11. C. J. Murphy, "Optical sensing with quantum dots," Anal. Chem. **74**, 520A-526A (2002).
12. S. W. Bishnoi, C. J. Rozell, C. S. Levin, M. K. Gheith, B. R. Johnson, D. H. Johnson, and N. J. Halas, "All-optical nanoscale pH meter," Nano Lett. **6**, 1687-1692 (2006).
13. A. O. Govorov, and I. Carmeli, "Hybrid structures composed of photosynthetic system and metal nanoparticles: plasmon enhancement effect," Nano Lett. **7**, 620-625 (2007).
14. J. M. Slocik, F. Tam, N. J. Halas, and R. R. Naik, "Peptide-assembled optically responsive nanoparticle complexes," Nano Lett. **7**, 1054-1058 (2007).
15. R. D. Artuso, and G. W. Bryantt, "Optical response of strongly coupled quantum dot - Metal nanoparticle systems: Double peaked fano structure and bistability," Nano Lett. **8**, 2106-2111 (2008).
16. M. Pelton, "Modified spontaneous emission in nanophotonic structures," Nat. Photonics **9**, 427-435 (2015).
17. J. Dintinger, S. Klein, F. Bustos, W. L. Barnes, and T. W. Ebbesen, "Strong coupling between surface plasmon-polaritons and organic molecules in subwavelength hole arrays," Phys. Rev. B **71,** 035424 (2005).
18. Y. B. Zheng, B. K. Juluri, L. L. Jensen, D. Ahmed, M. Q. Lu, L. Jensen, and T. J. Huang, "Dynamic tuning of plasmon-exciton coupling in arrays of nanodisk-j-aggregate complexes," Adv. Mater. **22**, 3603-3607 (2010).
19. E. Prodan, C. Radloff, N. J. Halas, and P. Nordlander, "A hybridization model for the plasmon response of complex nanostructures," Science **302**, 419-422 (2003).
20. M. Rahmani, B. Luk'yanchuk, and M. H. Hong, "Fano resonance in novel plasmonic nanostructures," Laser Photon. Rev. **7**, 329-349 (2013).
21. N. Large, L. Saviot, J. Margueritat, J. Gonzalo, C. N. Afonso, A. Arbouet, P. Langot, A. Mlayah, and J. Aizpurua, "Acousto-plasmonic hot spots in metallic nano-objects," Nano Lett. **9**, 3732-3738 (2009).
22. H. Wang, Y. L. Ke, N. S. Xu, R. Z. Zhan, Z. B. Zheng, J. X. Wen, J. H. Yan, P. Liu, J. Chen, J. C. She, Y. Zhang, F. Liu, H. J. Chen, and S. Z. Deng, "Resonance coupling in silicon nanosphere-j-aggregate heterostructures," Nano Lett. **16**, 6886-6895 (2016).
23. A. I. Kuznetsov, A. E. Miroshnichenko, M. L. Brongersma, Y. S. Kivshar, and B. Luk'yanchuk, "Optically resonant dielectric nanostructures," Science **354**, aag2472 (2016).
24. P. Albella, M. A. Poyli, M. K. Schmidt, S. A. Maier, F. Moreno, J. J. Sáenz, and J. Aizpurua, "Low-loss electric and magnetic field-enhanced spectroscopy with subwavelength silicon dimers," J. Phys. Chem. C **117**, 13573-13584 (2013).
25. A. B. Evlyukhin, S. M. Novikov, U. Zywietz, R. L. Eriksen, C. Reinhardt, S. I. Bozhevolnyi, and B. N. Chichkov, "Demonstration of magnetic dipole resonances of dielectric nanospheres in the visible region," Nano Lett. **12**, 3749-3755 (2012).
26. A. I. Kuznetsov, A. E. Miroshnichenko, Y. H. Fu, J. Zhang, and B. Luk'yanchuk, "Magnetic light," Sci. Rep. **2,** 492 (2012).
27. V. Rutckaia, F. Heyrot, A. Novikov, M. Shaleev, M. Petrov, and J. Schilling, "Quantum dot emission driven by mie resonances in silicon nanostructures," Nano Lett. **17**, 6886-6892 (2017).

28. A. E. Miroshnichenko, A. B. Evlyukhin, Y. F. Yu, R. M. Bakker, A. Chipouline, A. I. Kuznetsov, B. Luk'yanchuk, B. N. Chichkov, and Y. S. Kivshar, "Nonradiating anapole modes in dielectric nanoparticles," Nat. Commun. **6**, 8069 (2015).
29. J. A. Parker, H. Sugimoto, B. Coe, D. Eggena, M. Fujii, N. F. Scherer, S. K. Gray, and U. Manna, "Excitation of nonradiating anapoles in dielectric nanospheres," Phys. Rev. Lett. **124**, 097402 (2020).
30. K. V. Baryshnikova, D. A. Smirnova, B. S. Luk'yanchuk, and Y. S. Kivshar, "Optical anapoles: concepts and applications," Adv. Opt. Mater. **7**, 1801350 (2019).
31. V. A. Fedotov, A. V. Rogacheva, V. Savinov, D. P. Tsai, and N. I. Zheludev, "Resonant transparency and non-trivial non-radiating excitations in toroidal metamaterials," Sci. Rep. **3**, 2967 (2013).
32. V. Savinov, N. Papasimakis, D. P. Tsai, and N. I. Zheludev, "Optical anapoles," Commun. Phys. **2**, 69 (2019).
33. K. Koshelev, G. Favraud, A. Bogdanov, Y. Kivshar, and A. Fratalocchi, "Nonradiating photonics with resonant dielectric nanostructures," Nanophotonics **8**, 725-745 (2019).
34. U. Manna, H. Sugimoto, D. Eggena, B. Coe, R. Wang, M. Biswas, and M. Fujii, "Selective excitation and enhancement of multipolar resonances in dielectric nanospheres using cylindrical vector beams," J. Appl. Phys. **127**, 033101 (2020).
35. S. D. Liu, J. L. Fan, W. J. Wang, J. D. Chen, and Z. H. Chen, "Resonance coupling between molecular excitons and nonradiating anapole modes in silicon nanodisk-j-aggregate heterostructures," ACS Photon. **5**, 1628-1639 (2018).
36. A. F. Oskooi, D. Roundy, M. Ibanescu, P. Bermel, J. D. Joannopoulos, and S. G. Johnson, "MEEP: A flexible free-software package for electromagnetic simulations by the FDTD method," Comput. Phys. Commun. **181**, 687-702 (2010).
37. D. G. Hall, "Vector-beam solutions of Maxwell's wave equation," Opt. Lett. **21**, 9-11 (1996).
38. Q. Zhan, "Cylindrical vector beams: from mathematical concepts to applications," Adv. Opt. Photon. **1**, 1-57 (2009).
39. R. Dorn, S. Quabis, and G. Leuchs, "Sharper focus for a radially polarized light beam," Phys. Rev. Lett. **91**, 233901 (2003).
40. K. C. Toussaint, S. Park, J. E. Jureller, and N. F. Scherer, "Generation of optical vector beams with a diffractive optical element interferometer," Opt. Lett. **30**, 2846-2848 (2005).
41. M. Stalder, and M. Schadt, "Linearly polarized light with axial symmetry generated by liquid-crystal polarization converters," Opt. Lett. **21**, 1948-1950 (1996).
42. Y. Zhang, P. Li, C. Ma, S. Liu, H. Cheng, L. Han, and J. Zhao, "Efficient generation of vector beams by calibrating the phase response of a spatial light modulator," Appl. Opt. **56**, 4956-4960 (2017).
43. M. Kasperczyk, S. Person, D. Ananias, L. D. Carlos, and L. Novotny, "Excitation of magnetic dipole transitions at optical frequencies," Phys. Rev. Lett. **114**, 5 (2015).
44. U. Manna, J.-H. Lee, T.-S. Deng, J. Parker, S. Shepherd, Y. Weizmann, and N. F. Scherer, "Selective induction of optical magnetism," Nano Lett. **17**, 7196 (2017).
45. P. Wozniak, P. Banzer, and G. Leuchs, "Selective switching of individual multipole resonances in single dielectric nanoparticles," Laser Photon. Rev. **9**, 231-240 (2015).
46. L. Wei, Z. Xi, N. Bhattacharya, and H. P. Urbach, "Excitation of the radiationless anapole mode," Optica **3**, 799-802 (2016).
47. T. Das, and J. A. Schuller, "Dark modes and field enhancements in dielectric dimers illuminated by cylindrical vector beams," Phys. Rev. B **95**, 201111(R) (2017).
48. J. Sancho-Parramon, and S. Bosch, "Dark modes and fano resonances in plasmonic clusters excited by cylindrical vector beams," ACS Nano **6**, 8415-8423 (2012).
49. A. Yanai, M. Grajower, G. M. Lerman, M. Hentschel, H. Giessen, and U. Levy, "Near- and far-field properties of plasmonic oligomers under radially and azimuthally polarized light excitation," ACS Nano **8**, 4969-4974 (2014).
50. A. V. Failla, H. Qian, A. Hartschuh, and A. J. Meixner, "Orientational imaging of subwavelength au particles with higher order laser modes," Nano Lett. **6**, 1374-1378 (2006).
51. G. Bautista, M. J. Huttunen, J. Makitalo, J. M. Kontio, J. Simonen, and M. Kauranen, "Second-harmonic generation imaging of metal nano-objects with cylindrical vector beams," Nano Lett. **12**, 3207-3212 (2012).
52. X. Xie, Y. Chen, K. Yang, and J. Zhou, "Harnessing the point-spread function for high-resolution far-field optical microscopy," Phys. Rev. Lett. **113**, 263901 (2014).
53. Q. W. Zhan, "Trapping metallic Rayleigh particles with radial polarization," Opt. Express **12**, 3377-3382 (2004).
54. H. Cheng, P. Li, S. Liu, P. Chen, L. Han, Y. Zhang, W. Hu, and J. Zhao, "Vortex-controlled morphology conversion of microstructures on silicon induced by femtosecond vector vortex beams," Appl. Phys. Lett. **111**, 141901 (2017).
55. M. Mansuripur, "Distribution of light at and near the focus of high-numerical-aperture objectives," J. Opt. Soc. Am. A **3**, 2086-2093 (1986).
56. S. Rudin, and T. L. Reinecke, "Oscillator model for vacuum Rabi splitting in microcavities," Phys. Rev. B **59**, 10227-10233 (1999).
57. K. Hennessy, A. Badolato, M. Winger, D. Gerace, M. Atatüre, S. Gulde, S. Fält, E. L. Hu, and A. Imamoğlu, "Quantum nature of a strongly coupled single quantum dot–cavity system," Nature **445**, 896-899 (2007).

58. R. Chikkaraddy, B. de Nijs, F. Benz, S. J. Barrow, O. A. Scherman, E. Rosta, A. Demetriadou, P. Fox, O. Hess, and J. J. Baumberg, "Single-molecule strong coupling at room temperature in plasmonic nanocavities," Nature **535**, 127-130 (2016).